

DOI: 10.1002/adem.201300089

Generating Lithographically-Defined Tunable Printed Structural Color**

By Benjamin Michaelis, David R. E. Snoswell, Nicholas A. W. Bell, Peter Spahn, Goetz P. Hellmann, Chris E. Finlayson and Jeremy J. Baumberg*

We present a tunable method for generating lithographically defined printed structural color. Colloidal polymeric particles in suspension are assembled into strings in an electric field, with the field strength determining the spacing between neighboring strings, and thus the lattice spacing of these three-dimensional photonic crystals. Transient field-tuning thus results in both spectroscopic and visual changes to the structural color of the material. By using an organic UV-curable continuous matrix, we demonstrate that these tunable structures can be permanently fixed in a flexible polymer matrix and thus are suitable for printing applications, with no requirement for a “wash-out” step.

Synthetic photonic crystals are frequently produced using monodisperse colloidal particles crystallized into ordered arrays.^[1–3] Tunable structural color using these arrays has been explored previously for display devices^[4] but examples of rapidly assembled, permanent structural color materials suitable for printing applications are rare. Ideally, structural colored material for printing applications would use particles of one size to generate all colors (a single tunable “ink”), employ self-assembly in a sub-second timescale process and produce material which is flexible. Recent studies have focused on the use of magnetic fields to form strings of superparamagnetic colloidal particles showing structural color, which are then fixed in place by UV curing their surrounding matrix. Particle separation in these systems can be controlled by swelling the matrix with a hygroscopic salt^[5]

or adjusting the magnetic field strength before curing.^[6] The printing of a range of structural colors has been demonstrated by this technique; however, optical absorption by the magnetic particles, and the need for a “wash out” step of residual structural colors before printing, are noted as significant disadvantages of this technique.

Trau *et al.* have shown that DC and AC electric fields can assemble two-dimensional (2D) colloidal crystals between parallel plate electrodes,^[7] and developed electrohydrodynamic theory to explain long-ranged particle attractions.^[8] Whilst phase changes from random to crystalline order were reported upon varying the field strength, changes in lattice spacing were not observed. For three-dimensional (3D) assembly, crystallization can be driven by both electrohydrodynamic forces and induced dipole attractions, resulting in self-assembled 3D colloidal crystals displaying structural colour.^[9,10] Lumsdon *et al.* have also reported the use of dipole–dipole particle interactions for such assembly processes, when particles are concentrated near the electrodes.^[11] We have previously shown that this method can be extended to widely control lattice spacings in 2D colloidal crystals in aqueous suspensions by changes in field intensity.^[12] Critically, we showed that reversible lattice spacing changes of ~10% could be induced by changes in field intensity in under 100 ms, an order of magnitude faster than diffusion-limited gel-based techniques.^[4,13] However, the use of coplanar electrodes and relatively large particles (945 nm), produced visible color only by diffraction of transmitted light through particle strings in grating mode, rather than by Bragg reflection from a crystal structure which is the mechanism better suited to reflective displays. Induced, but photonically inactive 3D networks of particles have been demonstrated previously in studies of electro-rheological (ER) fluids, responding to electric fields at switching speeds of up to 1 ms for 10 μm particles^[14] and 0.2 ms for 21 nm aqueous latex suspensions.^[15] The exploitation of rapid self-assembly by electric fields for colloidal printed systems remains rather unexplored however.

In this paper, we demonstrate the formation and preservation of tunable crystal structures by ordering of colloids in an alternating electric field and subsequent UV curing of the organic dispersion medium. Hereby, we combine the parallel plate electrode cell geometry of ER studies^[14] with monodisperse sub-300 nm particle suspensions, to achieve rapidly assembled and tunable photonic

[*] Prof. J. J. Baumberg, B. Michaelis, Dr. D. R. E. Snoswell, N. A. W. Bell

Nano-Photonics Centre, University of Cambridge, Cambridge CB3 0HE, UK

E-mail: jjb12@cam.ac.uk

Dr. P. Spahn, Dr. G. P. Hellmann

Deutsches Kunststoff-Institut (DKI), Schlossgartenstrasse 6, D-64289 Darmstadt, Germany

Dr. C. E. Finlayson

Institute of Mathematical and Physical Sciences (IMAPS), Prifysgol Aberystwyth University, Wales SY23 3BZ, UK

[**] The authors thank Prof. Brian Vincent (University of Bristol, UK) and Dr. Chris Bower (Nokia Research Cambridge) for helpful discussions. This work was supported by UK EPSRC Grants EP/G060649/1, EP/G037221/1 (Nano DTC), and EP/H027130/1. Supporting Information is available from the Wiley Online Library or from the author.

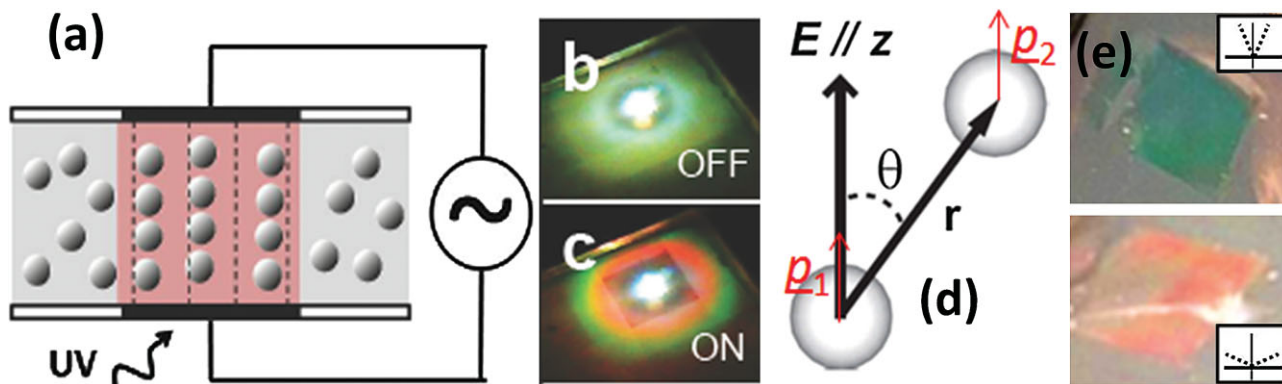


Fig. 1. (a) Schematic of AC field alignment inside cells consisting of parallel plate ITO electrodes encapsulating the monodisperse particle suspension. The electric field (dashed lines) induces chaining forces and self-assembly of particles into strings. (b,c) Macroscopic images of cells illuminated from above at normal incidence with the electric field off (b) and on (c) showing structural color due to particle strings. (d) Configuration of dipole interactions. (e) Iridescence of a cured colloidal crystal ($\approx 3 \text{ mm} \times 3 \text{ mm}$). Insets show viewing and illumination angles (dashed line) versus sample surface (horizontal line).

crystals with Bragg reflectivity at visible wavelengths. Vivid structural colors can be generated from one and the same ink by simple tuning of the applied electric field strength (“One-Pot Color”). Without the external stimulus, polymer particles are distributed randomly in the suspension, which forms a transparent film upon exposure to UV light such that no “wash-out” step is necessary. Hence, we show that the structures can be assembled and fixed in a flexible matrix, providing proof-of-principle demonstration of a structural color printing system.

The particle interactions here are derived from electrically induced dipoles and, thus we avoid using light-absorbing magnetic particles. The tunable dynamic structures produced use colloidal particles, composed of a polystyrene methacrylic acid co-polymer (PSMMA), synthesized by a standard surfactant-free emulsion polymerization technique.^[16] Particles synthesized in aqueous suspension are transferred to a fluid of poly(ethylene glycol) diacrylate monomer (PEGDA), via an ethanol solvent intermediate. Water is removed as an azeotrop with ethanol by gentle heating ($50\text{--}60^\circ\text{C}$) under reduced pressure. Excess ethanol is removed by forced air convection at room temperature to enhance evaporation and obtain suspensions with 67 wt% monomer, 10 wt% ethanol, and 23 wt% particles with size $248 (\pm 20) \text{ nm}$. To enable UV curing, 10% wt. of the free radical photo-initiator 2,2-dimethoxy-2-phenylacetophenone (DMPA) is added. Particle suspensions are then deionized by contact with mixed bed ion exchange resin (Amberlite MB150) until conductivity of the suspension is below $0.6 \mu\text{S cm}^{-1}$, subsequently the electrolyte concentration is fixed at 0.02 mM by addition of KCl. 10 mL quantities of suspension are sandwiched between glass microscope slides with lithographically patterned, parallel-plate ITO electrodes separated by a $25 \mu\text{m}$ gap set by a non-reactive gasket. Electrodes attached to an AC voltage source [Figure 1(a)] are driven with a sinusoidal voltage at 200 kHz, generating field strengths up to $1.6 \text{ MV}_{\text{RMS}} \text{ m}^{-1}$. The UV curing step is performed using a UV light emitting diode (Farnell 370 nm) placed 1 cm from the surface for 30 s.

For the assembly step, a droplet of suspension is placed on one electrode, encapsulated with the second electrode and gasket to create a cell with defined electrode separation (see Figure 1). At this stage the suspension in the cell appears milky due to scattering of the suspended particles. On applying the electric field the suspension between the electrodes becomes colored within a fraction of a second, with color controlled by the field strength [(Figure 1(b,c)]. Removing the electric field immediately results in a loss of color and these on and off states can be repeatedly cycled (tested for tens of minutes). When illuminated with a UV light the suspension in the cell solidifies within 10 s and the colored or non-colored state of the suspension remains permanently “frozen” in place regardless of any further switching of the electric field. Once the suspension has been cured in this way, the electrodes can be peeled off allowing removal of the solidified suspension containing structurally colored regions where the electric field was applied [Figure 1(e)].

The particle ordering we exploit is based on inducing electrical dipoles inside each particle which interact in a complex way with each other, and the surrounding solvent charges. At its heart is the dipole–dipole interaction [Figure 1(d)] and, as we show below, the particles assemble rapidly into long chains and these chains are then attracted into a stacked 3D array. The ability to UV cure the films and freeze the string structures permanently in place is achieved by using a low viscosity monomer, combined with a UV activated initiator, and the proven curing method of Kim *et al.*^[6] However, the challenge has been to develop particles which both remain stable in the monomer fluid, and which develop sufficient dipole intensity to form chains at achievable field strengths (without degradation of the ITO electrodes or dielectric breakdown). High surface conductivity is the most important factor in achieving strong electrically induced dipoles,^[17] so particles with methacrylic acid co-polymer were used to maximize surface charge. We note that charging phenomena in non-aqueous media can be complex and a full description of the nature of particle surface charge is beyond the scope of the current study.

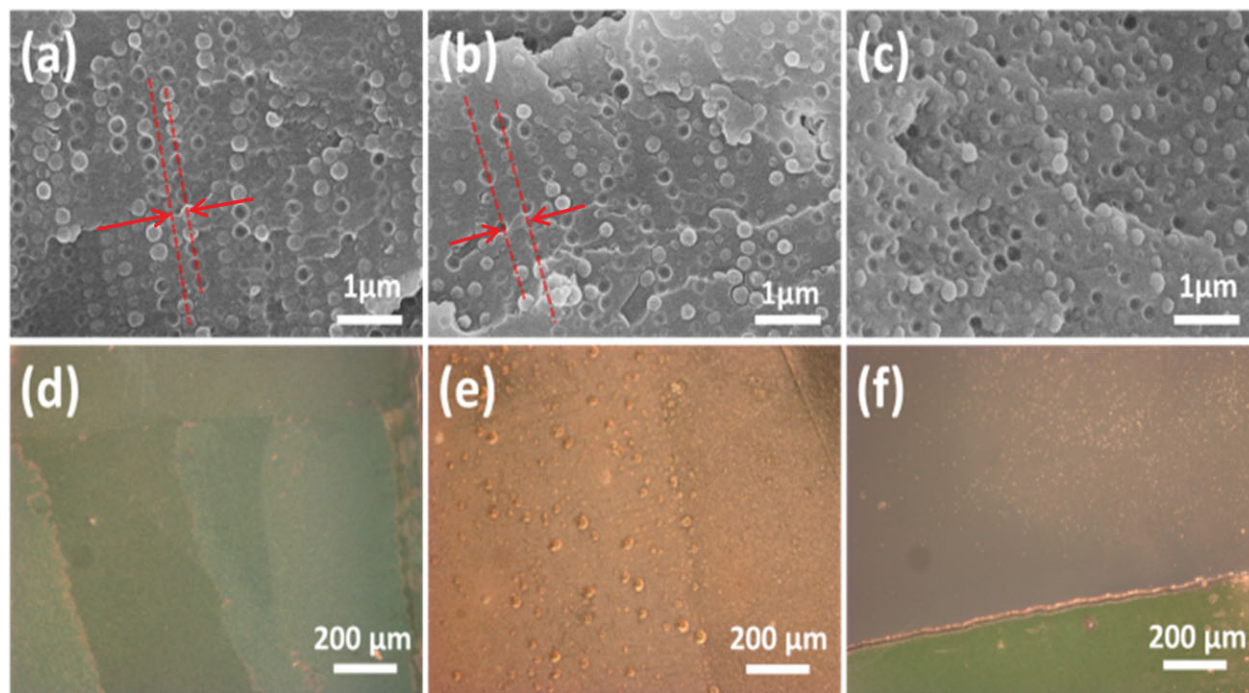


Fig. 2. (a)–(c) SEM images of cured particle suspensions in cross-section, with the applied fields being (a) $1.6 \text{ MV}_{\text{RMS}} \text{ m}^{-1}$, (b) $0.8 \text{ MV}_{\text{RMS}} \text{ m}^{-1}$, where the particles are visibly arranged into chains of increasing separation, and (c) zero, where the particles are randomly dispersed by Brownian motion. The spacing between representative adjacent strings is indicated by the dashed red lines in (a), where the spacing is $\approx 300 \text{ nm}$, and (b), where it is $\approx 450 \text{ nm}$. (d)–(f) show commensurate dark-field optical microscopy images of cured samples, with the applied fields being (d) $1.6 \text{ MV}_{\text{RMS}} \text{ m}^{-1}$ and (e) $0.8 \text{ MV}_{\text{RMS}} \text{ m}^{-1}$. (f) Shows the transition in color between a region of zero applied field (top) and a region where the field was $\approx 1.4 \text{ MV}_{\text{RMS}} \text{ m}^{-1}$ (bottom). For the microscopy measurements, an objective with $\times 5$ magnification and a dark-field acceptance angle of 9° was used.

Free-standing UV cured films were characterized by scanning electron microscopy (SEM) and optical microscopy. Cross-sections were obtained by embedding freestanding films in wax for microtome cutting, then subsequently SEM imaging. Figure 2(a–c) clearly shows particle strings assembling along the applied electric field lines. The spacing between neighboring aligned strings is tuned by the magnitude of the field, and is consistent with the observed optical changes. Corresponding dark-field scattering images of the samples [Figure 2(d,e)] illustrate a commensurate change in the observed structural color as the applied field is varied. Such images clearly show a well-defined boundary between regions containing strings and no strings [Figure 2(f)], demonstrating a lateral resolution of field patterning below $25 \mu\text{m}$ (the cell thickness).

Samples were also optically characterized using a collimated white light laser source (Fianium, spot size $\approx 100 \mu\text{m}$) and spectrometer. In Figure 3 we demonstrate how the structural color effects are tunable as a function of the applied field. At fixed illumination and detection angles, the spectral peak of dynamic string structures red-shifts and broadens as the voltage is decreased [Figure 3(a)]. Analyses of SEM images confirm that this field-induced red-shifting is fully correlated to increasing lateral spacing between the particle strings (“inter-string”), due to the decreased dipole strength.^[14,16] This highlights the contrast to previous studies in aqueous electrolytes, where changes in the particle–particle separation within strings (“intra-string”) was identified as the spectral tuning mechanism.^[12]

To elucidate these observations we now develop a simple model. The detailed description of electrically induced chaining is well known,^[17,18] and for clarity a qualitative description is provided here. Applying an alternating electric field across the particle suspensions electrically induces instantaneous dipoles in the particles due to a contrast in conductivity and dielectric constant between the particles and the surrounding fluid. Dipoles of adjacent particles attract each other in the direction of the field lines causing diffusing particles to lock into chains aligned with the electric field. Particles within the chains are charged and electrostatically repel each other at close surface separations. The balance between electrostatic repulsion and dipole attraction results in particle surface separations corresponding to a secondary minimum in the interaction potential. The particle–particle surface separation, which is determined by the secondary minima, can be controlled by the strength of the electric field and resulting dipole–dipole attraction.^[17] The total interaction potential for two particles is described as

$$V_{\text{total}}(\mathbf{r}) = \frac{p_1 p_2}{4\pi\epsilon_m \epsilon_0 |\mathbf{r}|^3} (1 - 3\cos^2\theta) + V_Y(\mathbf{r}), \quad (1)$$

where the first term arises from the two equal field-induced dipoles and the second arises from the effects of charge screening by counter-charges in the electrolyte which are accounted for by an exponential Yukawa potential, V_Y . Here θ is the angle between separation vector \mathbf{r} of the dipoles with moments p_1 and p_2 , which are both oriented along the electric field [see Figure 1(d)]. Increasing field strength draws

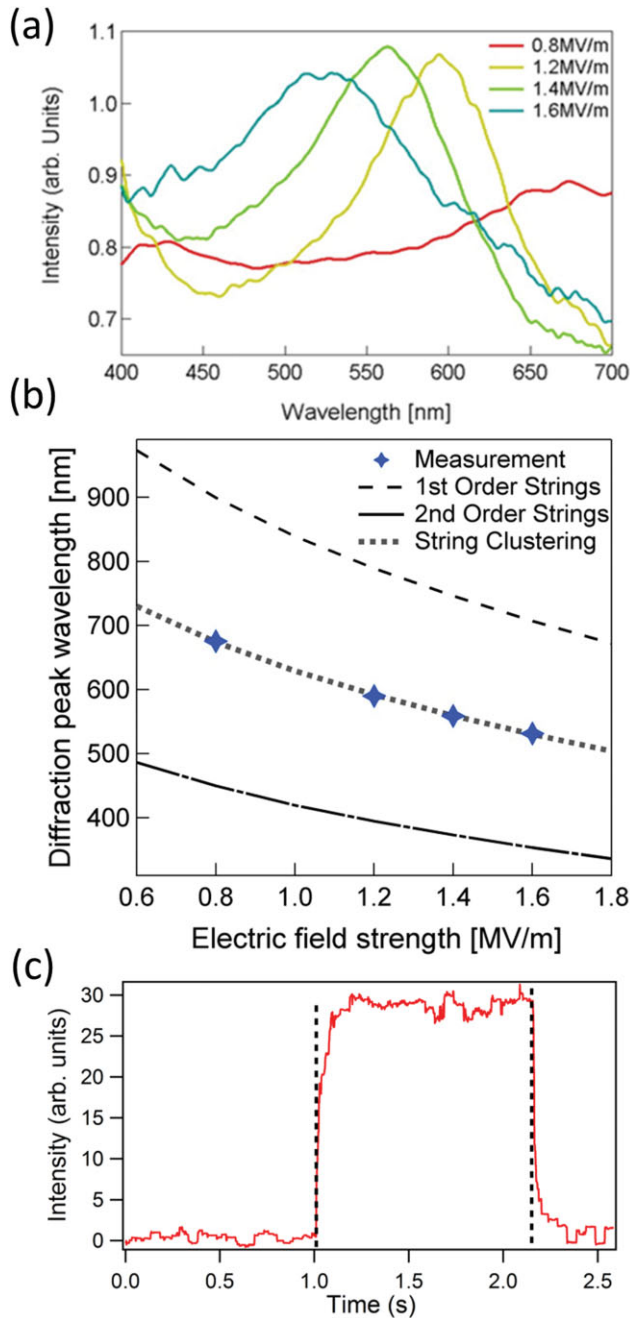


Fig. 3. (a) Dark field reflection spectra of colloidal crystals cured at various effective field strengths of $0.8\text{--}1.6\text{ MV}_{\text{RMS}}\text{ m}^{-1}$. (b) Comparison of experimentally measured peak scattering λ after UV curing with theoretical models, as a function of the electric field strength. The data (crosses) fit our model in which string clustering is the origin of tunable color, rather than the first and second order diffraction effects from particle separations within strings. (c) Dynamics of sample structural color. Applied electric field switches on/off at times indicated by dashed lines (no UV illumination). Red signal intensity is shown, extracted from RGB-format video images of a region within the electrodes. Corresponding video footage is available in the Supporting Information.

particles closer together, whilst lowering the field strength causes them to separate until, below a threshold field strength, the particles are no longer locked together and diffuse freely [see Figure 1(a)].

However, the separation of particles inside each string is not responsible for the structural color here. Instead, in a

higher order process, the average dipole-dipole attraction between individual strings leads to their 2D side-by-side alignment, hence forming 3D colloidal crystals. This attractive force between strings is comparatively low, as the particle dipole moments are screened by adjacent particles and the interface charges are geometrically further apart. The weaker attraction between particles in adjacent strings results in higher separations and the alignment process is slower. For the particle suspensions used for printing, formation of 2D arrays of vertical strings into photonic crystals is the dominant source of structural color, as demonstrated by the optical and structural analysis. The color is thus controlled by the separation of strings, which can be described by the same DLVO theory,^[19] but now including screened potentials. These can be described by summing the interaction potentials between one particle and its nearest neighbors within an adjacent particle string. We note that at small separations of particles within individual strings, the electric field acting on a particle is significantly modified by surrounding particles. To account for this effect, we use the local electric field strength from simulations by Martin *et al.*^[20] in our modeling. By minimizing the potential energy function of Equation 1 with respect to distance, numerical predictions for the equilibrium separation of adjacent particle strings are obtained, and hence predictions of the resonant peak λ , as a function of applied field. The relevant parameters included (detailed in Supporting Information Table S1) relate to the particle properties, the electrolyte and the applied electric field. As the ionic strength and the particle charge are not known precisely, they need to be fitted in the model. The numerical results presented in Figure 3(b) show good agreement with the experimental results. By contrast, the predicted resonant peaks for diffraction effects within strings do not correspond with the observed tunable colors; the first and second order peaks being in the UV/blue and near-IR regions of the spectrum, respectively. As a clear demonstration of the inter-string origin of structural color, the iridescent samples display different colors when observed under different angles [Figure 1(e)]. Notably, the sample color shows a red-shift with increasing incidence angle, which contradicts the Bragg–Snell law, if a simple multilayer structure is assumed (using the “intra-string” particle periodicity).^[21] The explanation for this is indeed that the visible structural color does not arise from particle strings normal to the substrate, but by *in-plane* diffraction from the lateral 2D colloidal crystal, as determined by the inter-string spacing.

SEM pictures show that the randomly dispersed colloids order into colloidal crystals, after application of a uniaxial electric field (see Figure 2); the particle separation after matrix shrinkage is in the order of the particle size at about 210–250 nm, whereas the inter-string spacing is seen to be field-tunable in the range of 300–500 nm. Thus using the Bragg–Snell equation for the average refractive index of 1.49, the diffracted wavelength of the particle chains is expected to be in the red or near-infrared region for observation at normal incidence. The second order diffraction should then be in the



Fig. 4. Three samples exhibiting lithographically patterned structural-color, as observed (a) in transmission under white-light illumination, (b) in reflection at an angle of $\sim 45^\circ$, and (c) reflection at close to normal incidence. The samples were made using a two-step method, consisting of electric field assembly and UV curing each under different field strengths. A shadow mask, covering parts of the suspension from UV light during the first curing step, was used to imprint the images. As a guide to scale, the printed patterns and text are all around 5 mm in height.

UV region. Green color can thus never be diffracted from particle chains and can only arise from other crystal plane orientations not present unless the chains order laterally. The green structural color thus arises from diffraction off the tilted planes produced by alignment of the strings; the estimated string-spacings, of 300 nm at $1.6 \text{ MV}_{\text{RMS}} \text{ m}^{-1}$ and 450 nm at $0.8 \text{ MV}_{\text{RMS}} \text{ m}^{-1}$, also give a good qualitative match with the experimentally observed diffraction peaks at 530 and 675 nm, respectively. Furthermore, the color arising purely from the inter-particle separation can be seen experimentally, both at very low and at very high field strengths, when the field is applied for long times prior to curing (Supporting Information, Figure S1). At low field strength the second order diffraction of the chains is just in the visible region, showing a blue color [Supporting Information Figure S1(a)]. At high field strengths the particles come close enough to each other for the diffracted light to be just at the upper end of the visible spectrum. This can be seen in Figure S1(b) of Supporting

Information, where red color evolves from particle strings within in larger domains of particles, which are expected to have high local electric field strengths.

In the context of potential applications, a particular point of interest is the dynamics of crystal formation. The structure formation occurs on two key timescales, depending upon the speed of particle string formation and the speed at which the strings assemble together. Whilst the former process is expected to match the sub-millisecond timeframes observed in our earlier experiments, simulations by Martin *et al.* have shown that the clustering leading to 2D hexagonal alignment of strings occurs on a timescale of the order of milliseconds in the case of moderate particle concentrations.^[20] Video imaging of samples (see Supporting Information) as the applied field is switched places an upper limit on the speed of the assembly process, and hence the switching time of the observed structural color. Extracting the intensities of the regions of structural color within the electrodes from the

image frames in these videos provides switching dynamics plotted in Figure 3(c). The time-dependence is characterized by a fast response within the first recorded frame after switching (≤ 30 ms), and also a minor rise/decay component of sub-second timescale.

Finally, whilst some degree of curing of electric-field induced colloidal photonic crystals into long-lasting structures has been reported,^[22] here we achieve *lithographically-patterned structural color*. As a proof-of-principle demonstration of the capabilities of our technique, images of such patterns are shown in Figure 4. The two-colored iridescent samples show clearly distinguishable contrast between areas of high- and low-field strength at all angles of light illumination and observation. In addition to the subjectively vivid colors produced, the samples are visually stable over periods of months to years, and can be expected to be mechanically/elastically robust, given the standard material properties of the polymeric components.

In this paper, we have demonstrated the ability to generate structural color from self-assembled strings of colloidal particles. The self-assembly process is rapid, generating particle strings with tunable lattice spacing using standard polymer particles and electric fields, which are easy to implement and control. Crucially, we demonstrate that the electrically induced particle chains can be permanently fixed in a polymer matrix, thereby showing potential for a new scanning printing process. Detailed patterning of structural color is difficult to achieve, and we see possible applications of the developed technique for printing processes where iridescent, non-fading structural color is favorable, such as security printing on banknotes, passports, and certificates. As the crystal formation follows the external stimulus effectively instantaneously, and due to the straightforward handling of AC electric fields with no requirement for a “wash-out” step, the developed process is also potentially applicable in inkjet printers, where UV curable inks are commonly used already.

Received: March 19, 2013

Final Version: March 27, 2013

[1] D. J. Norris, Y. A. Vlasov, *Adv. Mater.* **2001**, *13*, 371.

[2] Y. W. Chung, I. C. Leu, J. H. Lee, M. H. Hon, *J. Cryst. Growth* **2005**, *275*, 2389.

- [3] C. E. Finlayson, P. Spahn, D. R. E. Snoswell, G. Yates, A. Kontogeorgos, A. I. Haines, G. P. Hellmann, J. J. Baumberg, *Adv. Mater.* **2011**, *23*, 1540.
- [4] A. C. Arsenault, D. P. Puzzo, I. Manners, G. A. Ozin, *Nat. Photon.* **2007**, *1*, 468.
- [5] J. Ge, J. Goebel, L. He, Z. Lu, Y. Yin, *Adv. Mater.* **2009**, *21*, 4259.
- [6] H. Kim, J. Ge, J. Kim, S. Choi, H. Lee, H. Lee, W. Park, Y. Yin, S. Kwon, *Nat. Photon.* **2009**, *3*, 534.
- [7] M. Trau, D. A. Saville, I. A. Aksay, *Science* **1996**, *272*, 706.
- [8] M. Trau, D. A. Saville, I. A. Aksay, *Langmuir* **1997**, *13*, 6375.
- [9] T. Gong, D. T. Wu, W. M. Marr, *Langmuir* **2003**, *19*, 5967.
- [10] A. Yethiraj, A. V. Blaaderen, *Nature* **2003**, *421*, 513.
- [11] S. O. Lumsdon, E. W. Kaler, J. P. Williams, O. D. Velev, *Appl. Phys. Lett.* **2003**, *82*, 949.
- [12] D. R. E. Snoswell, C. L. Bower, P. Ivanov, J. G. Rarity, B. Vincent, *New J. Phys.* **2006**, *8*, 267.
- [13] J. H. Holtz, S. A. Asher, *Nature* **1997**, *389*, 829.
- [14] V. M. Zamudio, R. Nava, L. Rejon, M. A. Ponce, S. Viquez, V. M. Castano, *Physica A* **1996**, *227*, 55.
- [15] C. Chassagne, M. Fontana, G. J. M. Kopler, *Physica A* **2001**, *298*, 24.
- [16] J. W. Goodwin, J. Hearn, C. C. Ho, R. H. Ottewill, *Br. Polym. J.* **1973**, *5*, 347.
- [17] N. Elsner, C. P. Royall, B. Vincent, D. R. E. Snoswell, *J. Chem. Phys.* **2009**, *130*, 154901.
- [18] U. Dassanayake, S. Fraden, A. van Blaaderen, *J. Chem. Phys.* **2000**, *112*, 3851.
- [19] a) DVLO Theory, after Derjaguin, Landau, Verwey and Overbeek; b) E. J. W. Verwey, J. Th. G. Overbeek, in *Theory of the Stability of Lyophobic Colloids*, Elsevier, Amsterdam **1948**.
- [20] J. E. Martin, R. Anderson, C. P. Tigges, *J. Chem. Phys.* **1998**, *108*, 3765.
- [21] M. E. Leunissen, H. R. Vutukuri, A. van Blaaderen, *Adv. Mater.* **2009**, *21*, 3116.
- [22] A. Yetheraj, J. H. J. Thijssen, A. Wouterse, A. van Blaaderen, *Adv. Mater.* **2004**, *16*, 596.